Received: 25/ Jan / 2016
Accepted: 30/ Apr/ 2016

Fatigue Behavior of Heat Treated 30 MSV 6 Vanadium Micro alloyed Steel

M. Hajisafari [a,*], S. Nategh [b,*], H. Yoozbashizadeh [b], A. Ekrami [b]

[a] Department of Metallurgy and Materials Engineering, Yazd Branch, Islamic Azad University, Yazd, Iran

[b] Department of Materials Science and Engineering, Sharif University of Technology, Tehran, Iran

Abstract

Fatigue behavior of vanadium micro-alloy steel has been studied in this research. Here, microstructure constituents were considered which essentially are dependent on the heat treatment conditions. The results of high cycle fatigue tests revealed that heat treatment procedure and cooling rates have significant effects on fatigue properties. Optimal heat treatment cycle of the micro-alloyed steel was determined to be austenitizing at 950 °C for 1 h and air cooling to room temperature followed by aging at 600 °C for 1.5 h. Scanning Electron Microscopy (SEM) and Transmission Electron Microscopy (TEM) were utilized to characterize the microstructure of heat treated specimens so as to understand the effect of microstructure on fatigue behavior. The optimal heat treatment cycle resulted in significant improvement of fatigue strength due to the development of uniform distribution of fine precipitates in a refined microstructure. Further study based on the Basquin's equation showed that at a constant stress, maximum fatigue life belongs to the specimen, heat treated at the optimal condition. Furthermore, minimum fatigue life is related to the specimen cooled at the rate of 6.4 °C/s. In addition, at the constant value of fatigue life, the maximum and the minimum fatigue strengths are related to the optimally heat treated specimen and the specimen cooled at the rate of 6.4 °C/s, respectively.

Keywords: Micro-alloyed Steel, Heat Treatment, Microstructure, Fatigue, TEM

* Corresponding authors. Tel.: Tel.: +989131519498
E-mail addresses: hajisafari@iauyazd.ac.ir

1. Introduction

The mechanical properties of the micro-alloyed steels are favorable to both manufacturing and service performance of automotive components. Depending on deformation temperature, cooling rate and the chemical composition, a variety of microstructures in micro-alloyed steels can be obtained [1,2]. Heat treatment on the micro-alloyed steels is performed in order to obtain dual phase and multiphase microstructures. There have been detailed investigations on microstructural evolutions during different heat treatments and their influence on tensile behavior of micro-alloyed steels [3]. The strength, ductility and fatigue resistance of micro-alloyed steels can be attributed to their microstructural aspects [4,5].

Over the past two decades, research has been focused on the thermo-mechanical processing to enhance strength, toughness and fatigue strength of micro-alloyed steels. Numerous investigations have been carried out to determine the effect of microstructural evolution on fatigue behavior of micro-alloyed steels. These studies have usually separately characterized the effect of heat treatment on precipitates, microstructure and mechanical properties [3-7]. Although, the effect of heat treatment on fatigue behavior has been clarified, the influence of optimum cooling rate and ageing temperature on 30MSV6 micro-alloyed steel has not been extensively investigated in detail. It has only been shown for several micro-alloyed steels that fatigue behavior is quite different for microstructures produced under different forging and hot rolling conditions. For example, Laurito et al. [3] evaluated the effects of microstructure on fatigue crack growth behavior of the low carbon-manganese micro-alloyed steel. They demonstrated that the distinct microstructural conditions were obtained by means of inter critical and isothermal heat treatments followed by water quench, in which the material specimens were kept at the temperature of 800, 950 and 1200 °C. Singh et al [4] investigated the possibilities of achieving at least comparable mechanical properties and wear resistance to plain carbon R-19/93 grade coach and wagon wheel steel by suitable micro-alloying and heat treatment. They were found that normalized wheels properties such as endurance limits and wear resistance were superior to R-19/93 grade wheel.

Sankaran et al. [5] investigated the monotonic, cyclic stress-strain and low cycle fatigue behavior of 38MnSiVS5 micro-alloyed steel having different microstructures due to different forging conditions. Fatigue crack initiation and propagation mechanisms corresponding to different microstructural conditions have also been compared. Also, Sankaran et al. [6] investigated the high cycle fatigue behavior of 38MnSiVS5 micro-alloyed steel which had experienced controlled thermo-mechanical processing to generate a multiphase microstructure. The endurance limit, fatigue thresholds, crack growth and crack closure characteristics were identified.

Bhat and Fine [7] indicated that the initial formation of a fatigue crack as a nucleation process is due to random fluctuations of a meta-stable assembly of defect structures generated during cycling for a pure iron and a high strength low alloy steel produced by hot -rolling. Therefore, in the present study a new approach for optimization of fatigue behavior of the 30MSV6 vanadium micro-alloyed steel through precipitation hardening under various ageing and cooling conditions was studied. The effects of these conditions on microstructure and also mechanical properties such as ductility, yield and tensile strengths were characterized. Then the optimum treatment regarding a desirable combination of

ductility and yield strength was determined. Finally, fatigue behavior (i.e. crack initiation and S-N curve behaviors) of the specimen undergone the optimum condition of treatment was studied. Furthermore, TEM studies on microstructure and morphology of precipitates were carried out to illustrate the variation of mechanical properties with heat treatment conditions.

2. Experimental procedures

High strength micro-alloyed steel produced in Iran Alloy Steel Company, in the form of hot rolled and air cooled rods of 20 mm in diameter with the chemical composition shown in Table 1, was used. Tensile specimens with 20 mm gauge length were CNC-machined out according to ASTM-E8M standard [8]. The AC_3 temperature was calculated according to Andrews equation (equation 1) [9].

$$AC_3=910 - 203(C)\ ^{\wedge}0.5 - 15.2Ni + 44.7Si + 104V + 31.5Mo + 13.1W \quad (1)$$

That x is weight percent of x element. According to this equation austenitizing temperature was calculated 836 °C. Therefore, austenitizing temperatures were selected to be 900-980 °C. Austenitizing was carried out for 1 h in an electric furnace operating under argon atmosphere. Three different cooling rates such as cooling in air (AC), cooling in insulated stainless steel cylinder (ISSC) and cooling by fan (FC)were used for cooling. A data logger, which records the time and temperature during cooling, was used to measure the cooling rate. The cooling rates for FC, AC and ISSC were equal to 6.4 °C/s, 3.8 °C/s and 0.9 °C/s, respectively. In order to study the effect of aging temperature on precipitation and strengthening, aging treatment was carried out at 570–640 °C for 1.5 h (Fig1).

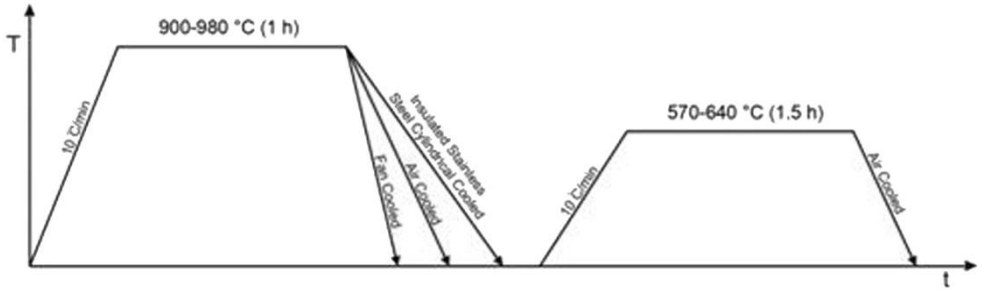

Fig1. Schematic diagram showing heat treatment process of specimens investigated

Specimens were then polished into fine surfaces and then Universal Testing Machine GOTECH GT–7001–LC30 was used with a constant head speed of 0.05 mm/min for tensile testing. The high cycle fatigue specimens were prepared according to ASTM-E466 standard [10]. After machining, emery papers of 320-3000 grit were used to polish the surface of specimens. To achieve a fine surface finish, specimens were finally polished by cotton. The high cycle fatigue test was carried out using SANTAM rotating-bending fatigue testing machine (SANTAM, ltd. IRAN) at different stress amplitudes.

Optical microscope and Scanning Electron Microscope (SEM, LEO 440i) were used for microstructural characterization. For etching of specimens, 2% Nital etchant was selected. A Digital image processor program was used to determine the pre-eutectoid ferrite size and pearlite interlamellar spacing. Transmission Electron Microscopy (TEM, 200kV, JEOL 2010) was carried out on specimens prepared by ion milling in order to study precipitates.

3. Results and discussion

In Fig 2 and Fig 3, the effect of different cooling rates on the microstructure, can be seen in optical and SEM micrographs of heat treated specimens, respectively. It can be seen in Fig. 2a that the as-received specimen represents pearlite and polygonal pre-eutectoid ferrite. Furthermore, microstructural studies revealed that increasing the cooling rate from austenitizing temperature results in the reduction of pre-eutectoid ferrite size. Similarly, Laurito et al. [3], Jahazi and Eghbali[11]reported the effect of cooling rate on the ferrite size in low carbon micro-alloyed steel and two micro-alloyed forging steels, respectively. As seen in Fig. 2, with an increase in the cooling rate, the equiaxed morphology of the pre-eutectoid ferrites in the as-received specimen (Fig. 2a) has been converted to a lath-type one (Fig. 2b-d).

This phenomenon is generally associated with the influence of cooling rate on the growth rates of ferrite [11]. A high cooling rate suppresses the $\gamma \rightarrow \alpha$ transformation and increases the nucleation rate of pre-eutectoid ferrite. Therefore, fan cooled specimen would be expected to give a finer microstructure compared to specimens cooled in air and insulated stainless steel cylinder. It is clear that, the $\gamma \rightarrow \alpha$ transformation occurs in two steps: nucleation and growth. During nucleation, a new interface is generated, which separates the product pre-eutectoid ferrite phase from the parent austenite phase.

This interface migrates into the surrounding parent phase during the subsequent growth. Cooling rate from austenitizing temperature affects the nucleation and growth phenomena. .Jahazi and Eghbali[12] showed similar results for the microstructure and properties of forged medium carbon micro-alloyed steels which had experienced cooling in different media such as air, sand and water.

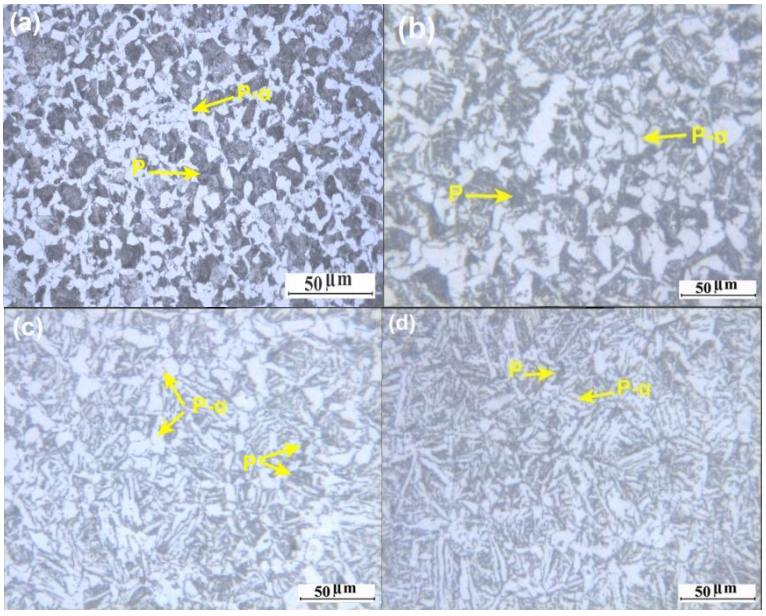

Fig2. Optical micrographs for specimens which experienced different cooling conditions; they were all austenitized at 950 °C for 1 h and aged at 600 °C for 1.5 h:As received; b) Cooled in insulated stainless steel cylinder; c) Air cooled; d) Fan cooled; P is pearlite and P-α is pre-eutectoid ferrite

As seen in Fig.3 and Table 2, the increasing in the cooling rate reduces the pearlite interlamellar spacing. As the cooling rate is increased, the under cooling is increased. Therefore, the driving force for transformation is increased which results in finer pearlite interlamellar spacing. To be more precise, increasing the cooling rate caused variation of diffusion kinetics. Generally, the slow diffusivity at low temperatures reduces the diffusion distance and consequently reduces the pearlite interlamellar spacing. Also, According to previous investigations, interlamellar spacing is directly dependent on the transformation temperature and inversely proportional to under-cooling below the eutectoid temperature [13]. The relationship between interlamellar spacing and transformation conditions is in accordance with the change in the growth rate.

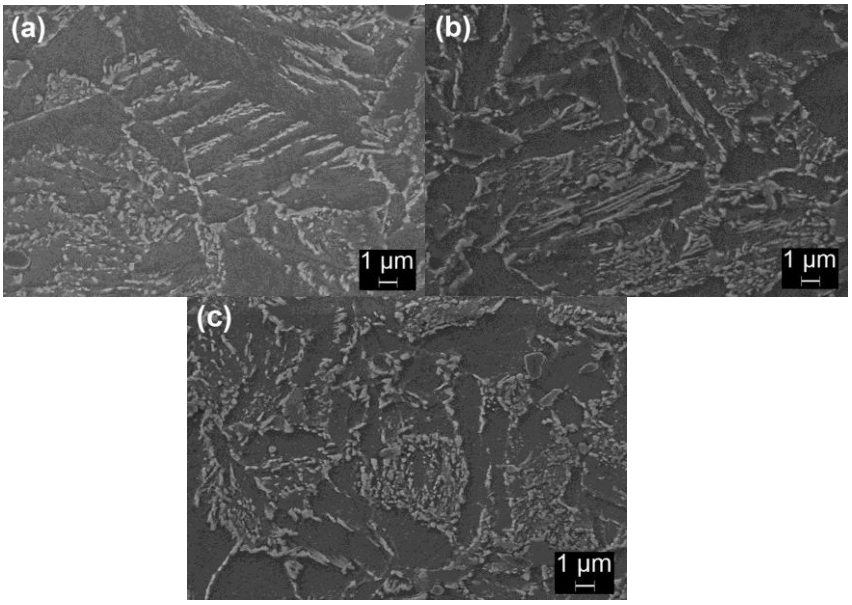

Fig3. SEM micrographs of specimens austenitized at 950 °C for 1 h, cooled at different rates and aged at 600 °C for 1.5 h: a) 0.9 °C/s; b) 3.8 °C/s; c) 6.4 °C/s

Table1. Chemical composition (wt. %) of the 30MSV6 micro alloyed steel

Elements	C	Si	Mn	P	S	Cr
Wt. %	0.3	0.54	1.47	0.0167	0.05	0.21
Elements	Mo	Ni	Al	V	Ti	N
Wt. %	0.005	0.10	0.022	0.11	0.017	≥0.012

The exact variations of matrix constituents versus heat treatment conditions and also the matrix constituents of the as-received specimen, together with their mechanical properties are presented in Table 2.As seen in this table, austenitizing temperatures did not influence on the microstructure and micro-constitutes of matrix. The steel contains 0.017 wt. % Ti which inhibits the growth of initial austenite grains during the process. Furthermore, a good combination off-tensile strength and ductility was obtained in the heat treated specimen according to the following conditions: Austenitizing at 950 °C for 1h, air cooling and ageing at 600 °C for 1.5h. This heat treatment cycle was selected as the optimal condition for the 30MSV6 micro-alloyed steel.

Table2. Microstructure specification and mechanical properties at different austenitization and aging temperatures (austenitizing time: 1 h and aging time: 1.5 h)

Characteristics		Pearlite interlamellar spacing(μm)	Pre-eutectoid ferrite size(μm)	Pre-eutectoid ferrite aspect ratio(%)	YS (MPa)	UTS (MPa)	El(%)	σ_Y / σ_{UTS}
As-received		0.268	2.54	27.58	648.9	807.8	14.3	0.803
Austenitizing Temperature (^oC)	Ageing Temperature (^oC)	Cooling Medium: ISSC						
900	570	0.217	2.19	16.29	664.6	809.4	18.1	0.821
	600	0.218	2.21	17.8	671.4	804.8	17.9	0.834
	640	0.210	2.25	16.02	667.3	801.9	17.4	0.832
950	570	0.221	2.39	16.90	646.5	779.2	16.25	0.835
	600	0.208	2.28	17.12	653.2	768.4	19.5	0.850
	640	0.213	2.36	15.93	652.4	750.8	17.5	0.869
980	570	0.219	2.42	16.23	628.4	721.6	17.3	0.871
	600	0.232	2.45	15.32	632.8	732.1	16.82	0.864
	640	0.209	2.45	15.84	610.3	709.7	16.9	0.860
Cooling Medium: AC								
900	570	0.128	1.79	21.12	704.2	821.8	16.8	0.857
	600	0.126	1.74	20.15	710	825.4	16.6	0.831
	640	0.124	1.84	21.21	694.4	819.8	17.3	0.847
950	570	0.145	1.92	20.29	680.3	772.9	18.7	0.880
	600	0.127	1.96	19.89	750.9	843.1	18.1	0.891
	640	0.141	1.95	20.04	639.1	781.6	19.2	0.818
980	570	0.130	1.99	19.78	653.2	765.2	18.8	0.854
	600	0.139	2.07	19.88	661.2	778.2	18.9	850
	640	0.127	2.10	20.14	643.7	770.6	17.8	0.835
Cooling Medium: FC								
900	570	0.100	1.21	25.94	684.5	815.2	15.9	0.840
	600	0.090	1.12	25.42	697	827.8	15.7	0.843
	640	0.101	1.17	26.32	663.3	800.2	15.3	0.829
950	570	0.102	1.23	24.91	678.5	800.4	16.1	0.848
	600	0.089	1.26	26.55	641.5	812.2	16	0.790
	640	0.091	1.25	24.29	635.2	788.2	15.4	0.806
980	570	0.103	1.40	25.74	671.4	749.1	15.8	0.896
	600	0.099	1.48	25.83	684.2	793.4	115.3	0.862
	640	0.110	1.43	24.12	664.7	765.3	15.4	0.869

In order to study the effect of microstructure on the mechanical properties, TEM studies were carried out on the optimal heat treated specimen. According to the TEM observations, three different precipitations such as; random precipitation, inter-phase precipitation, and heterogeneous precipitation on the dislocations were identified (Figs. 4 and Fig.5).These figures show bright field TEM micrographs of the specimen austenitized at 950 °C for 1 h, air cooled, and aged at 600 °C for 1.5 h. Figure4a shows precipitates formed within pre-eutectoid ferrites and phase boundaries. Figure5a indicates parallel sheets consisting of fine precipitates formed repeatedly with regular spacing placed on dislocations. The formation of precipitates on the dislocations can be explained by the

reduction of strain field energy between the precipitates and matrix [14-17]. Figure4b and Fig. 5b show the selected area diffraction patterns (SADP) of the precipitates indicated by arrow. Figure4c and Fig. 5c show EDS analyzes of precipitates shown in Fig. 4a and Fig. 5a. Figure4d and Fig. 5d show the SADP of the matrix around the precipitates in Fig. 4a and Fig. 5a. Figure4e and Fig. 5e show the EDS analyzes of matrix around the precipitates in Fig. 4a and Fig. 5a. The different parts of Fig. 4 and Fig. 5 revealed that: (I) Precipitates in this specimens are mainly (V, Ti)C (Fig. 4-b,c) and VC (Fig. 5-b,c).(II) The calculated lattice parameters of (V, Ti)C and VC are 4.34 Å and 4.26 Å, respectively. Furthermore, crystal structure of these carbides is a face centered cubic unit cell of NaCl type; that is in good agreement with previous reported ones [18].(III) The calculated lattice parameter and crystal structure of the matrix is 2.53 Å and body centered cubic, which indicates that the matrix is ferrite (Figs. 4-d,eand Figs. 5-d,e). (IV) The orientation relationship between pre-eutectoid ferrite and (V,Ti)C is a cube–cube one ($[111]_{\alpha}//[001]_{(V,Ti)C}$), and α/(V,Ti)C interface is non-coherent. Also, the orientation relationship between pre-eutectoid ferrite and VC is a cube–cube one ($[111]_{\alpha}//[001]_{VC}$) and α/VC interface is non-coherent.

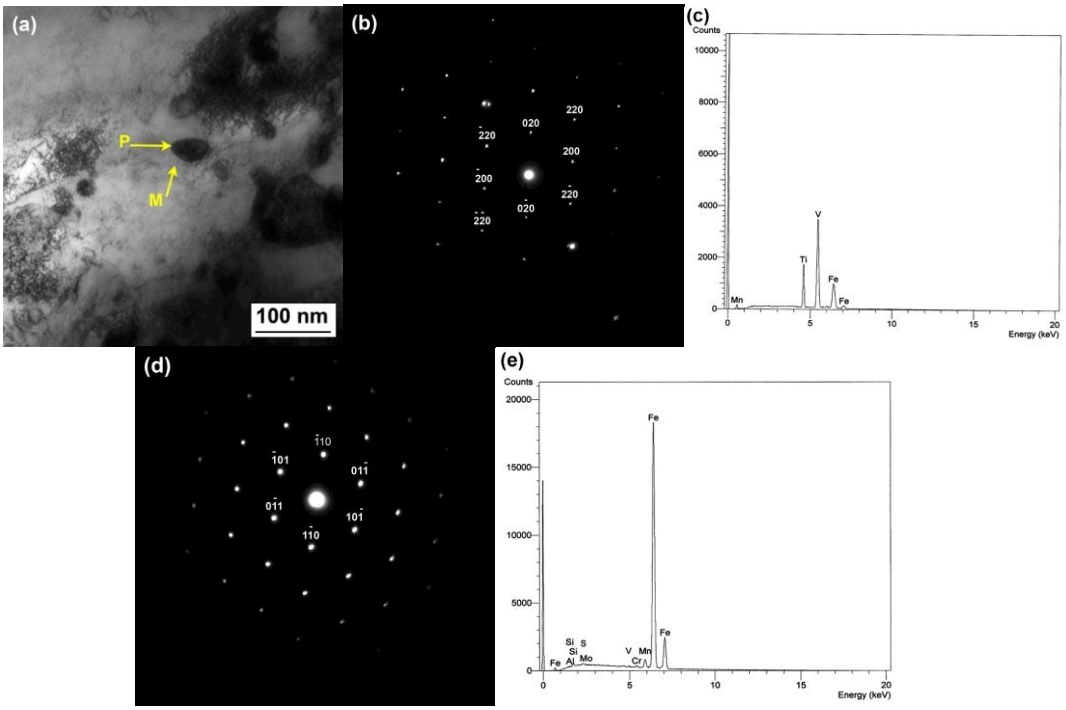

Fig4. a) Bright field TEM micrographs of fine precipitates distributed randomly in pre-eutectoid ferrite phase and at grain boundaries; b) SADP for the precipitate shown in image a (P-arrow); c) EDS analysis of the precipitate shown in image a (P-arrow); d) SAD pattern for the matrix around the precipitate shown in image a (M-arrow); e) EDS analysis of the matrix around the precipitate shown in image a (M-arrow)

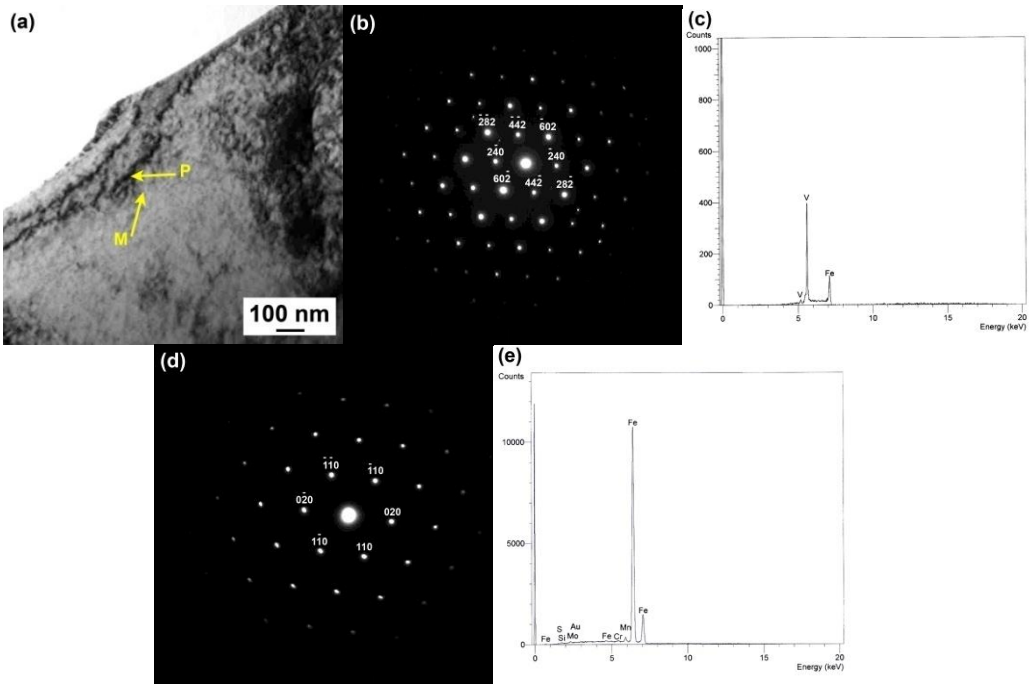

Fig5. a) Bright field TEM micrographs of fine precipitates heterogeneously nucleated on dislocations; b) SAD pattern for the precipitate shown in image a (P-arrow); c) EDS analysis of the precipitate shown in image a (P-arrow); d) SAD pattern for the matrix around the precipitate shown in image a (M-arrow); e) EDS analysis of the matrix around the precipitate shown in image a (M-arrow)

Improvement in the strength and ductility of optimal heat treated specimen can be related to the refinement in the pre-eutectoid ferrite size, interlamellar spacing of pearlite and the formation of precipitates at different sites of matrix as mentioned above, i.e. optimal heat treatment reduces the size of pre-eutectoid ferrite and interlamellar spacing of pearlite. Furthermore, during optimal heat treatment fine (V,Ti)C and VC precipitates form in the different sites of microstructure.

Fatigue behaviors of heat treated specimens austenitized at 950 °C, followed by different cooling rate and aged at 600 °C for 1.5h were presented in Fig. 6.Fatigue limit was defined for the air cooled specimens (optimal conditions) as the stress amplitude at which, failure did not occur up to 1.7×10^6 cycles. It was calculated to be 384MPa that was higher than the fatigue limit of the fan cooled specimens which was equal to 320MPa on the basis of 1.9×10^6 cycles. For the specimens cooled in the Insulated stainless steel cylinder, fatigue limit was determined to be 292 MPa, based on 2.8×10^6 cycles. The power law Basquin relationships were found to be valid for all the present heat treatment conditions and this behavior could be represented as:

$$\sigma=3589.219(N_f)^{-0.148} \quad (1)$$

$$\sigma=2238.721(N_f)^{-0.121} \quad (2)$$

$$\sigma=1990.673(N_f)^{-0.119} \quad (3)$$

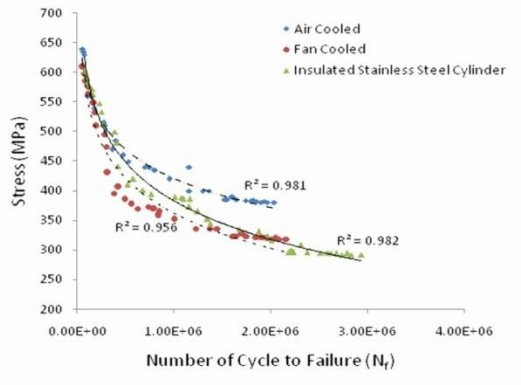

Fig6. S-N curves of 30MSV6

Vanadium micro alloyed steel considering all the conditions in the present study

This function is shown in Fig. 7. Comparison between fatigue life at constant stress: As shown in Figs. 7 and 6, at a constant stress, the maximum and the minimum fatigue life are related to the optimally heat treated specimen and the specimen cooled at the rate of 6.4 °C/s, respectively. For example, at a constant alternative stress of 400 MPa (log σa=2.602), $2N_f$ for the optimally heat treated specimen and specimen cooled at the rate of 0.9 °C/s is equal to 2749091 and 1519911, respectively. According to table 3, Basquin's relation coefficients for the fan cooled specimens are less than the considered values; hence, fatigue life has to be confined to the given values. According to the calculations, it was seen that fatigue life is 719686 for the fan cooled specimen. This is an unexpected value according to the data given during fatigue test (Fig. 6). It is a result of microstructure and indicates that a decrease in strength and ductility have a negative influence on fatigue life and strength.

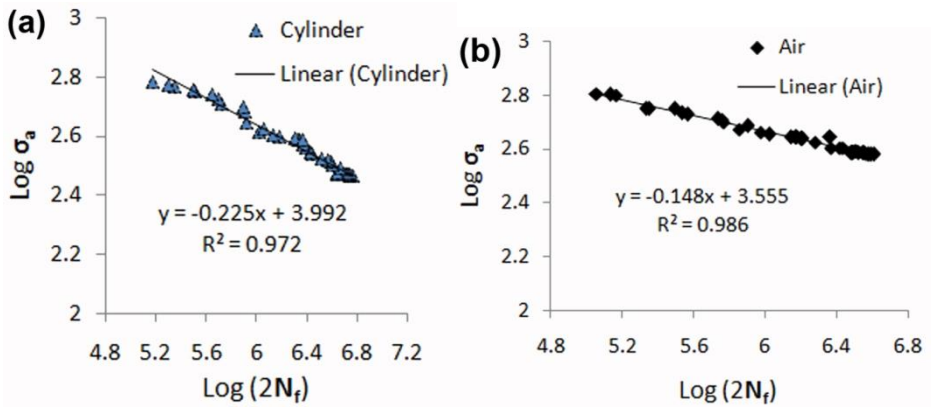

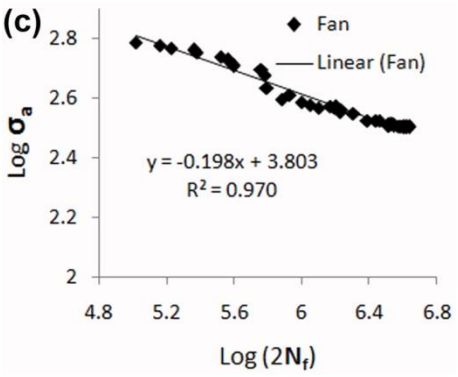

Fig7.Basquin's log-log relationship of fatigue specimen's austenitized at 950°C for 1 h, cooled at different media and aged at 600 °C for 1.5 h:a) Cooled in insulated stainless steel cylinder; b) Air cooled; c) Fan cooled

Additionally, fatigue life at an alternating stress of 400 MPa for the optimal specimen is 1.81 and 3.82 times to that of the specimen cooled at the rate of 0.9 and 6.4 °C/s, respectively. This increase in fatigue life for the optimal specimen is due to variation in microstructure constituents and the related mechanical properties, specially, increase in strength and ductility. Therefore, the fan cooled specimen has a higher ultimate tensile strength compared to the specimen cooled in insulated stainless steel cylinder but has a lower yield strength and ductility. It indicates the more significant effect of yield strength and ductility than the ultimate tensile strength on fatigue strength. (Ultimate tensile strength, yield strength and ductility for the fan cooled specimen and the specimen cooled in insulated stainless steel cylinder is 812.2 MPa, 653.2 MPa, 16.3% and 768.5 MPa, 661.5 MPa, 17.7%, respectively.)

Comparison in change of fatigue strength at constant fatigue life: As shown in Figs. 6 and 7, at a constant fatigue life, the higher value of fatigue strength is concerned to the optimal specimen and the lower value is for the fan cooled one. For example, at a constant fatigue life of 1000000 ($\log 2N_f$ =6), the fatigue strength (σ_a) for the optimal specimen, specimen cooled in insulated stainless steel cylinder and the fan cooled one are 464 MPa, 420 MPa and 384 MPa, respectively. So, the fatigue strength of the optimal specimen, increased to about 9.5 and 17.2% respectively in comparison to the specimen cooled in insulated stainless steel cylinder and the fan cooled one, while the increase in the ultimate tensile strength for this specimen, compared to the above mentioned specimens, is 9.7 and 3.8% respectively. Also, the increase in yield strength for the optimal specimen is 13.5 and 14.9%, comparing with the specimen cooled in insulated stainless steel cylinder and the fan cooled one, respectively. Therefore, it can be noted that at the fatigue life of 1000000, the value of increase in fatigue strength for the optimal specimen is about 0.98 and 4.5 times to that of the specimen cooled in insulated stainless steel cylinder and the fan cooled one, respectively. Cooling rates more than 3.8 °C/s, deleteriously affects the fatigue strength.

Finally, major factors to improve strength, ductility and fatigue behavior are pearlite interlamellar spacing, pre-eutectoid ferrite size and the formation of VC and (V,Ti)C precipitates at different sites of matrix as mentioned earlier.

It is worth noting that, the optimal heat treatment condition resulted in an improvement in the ultimate tensile strength, yield strength and ductility of 30MSV6

micro alloyed steel about 4.3%, 15.8% and 26.6%, respectively in comparison with the as-received specimen. Also, the fatigue limit of the specimen which had experienced optimum conditions of heat treatment was better than those of fan cooled specimens and specimens cooled in insulated stainless steel cylinder. This improvement in fatigue limit can be related to the less cyclic strain hardening present in the air cooled specimens (which are optimally heat treated ones)compared to other conditions. On the other hand, an increase in yield strength and ductility resulted in the improvement of fatigue limit and crack initiation resistance.

Figure8 shows the fractographs of the fatigue specimen which had been heat treated in optimal conditions. As shown in this figure, initiation of cracking happened in the surface of specimen (Fig. 8a).As shown in Fig.8b, propagation of fatigue crack in this specimen was predominant in the pre-eutectoid ferrite-pearlite microstructure through the ductile fracture mechanism of micro void coalescence and growth. The voids appeared to nucleate at precipitates where the continuity between the matrix and the second phase particles was relatively weak. Striation-like features can also be observed in this specimen (Fig. 8c). The composite microstructure, mixture of ferrite and pearlite phases, caused the discontinuous striation features in the ferrite-pearlite steel. On the other word, the least resistance path to fatigue crack growth was through the ferrite and the stronger pearlite colonies tended to retard the crack growth [5].

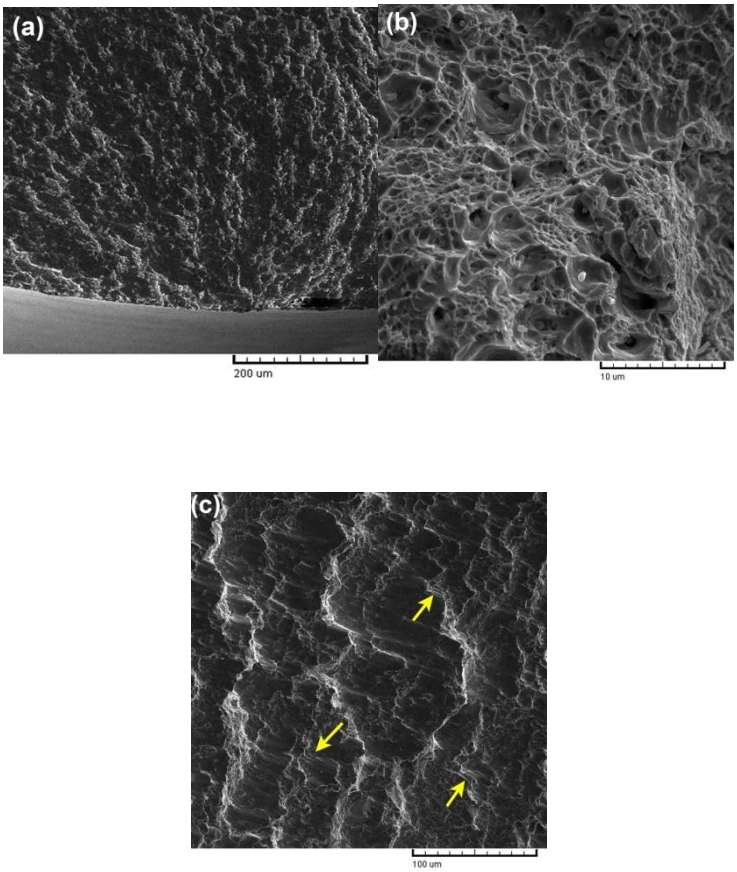

Fig8. SEM micrographs of room temperature fatigue fracture surface of the specimen austenitized at 950 °C for an hour, air cooled and finally aged at 600 °C for 1.5 ha) Crack initiation in the surface; b) Ductile fracture mechanism of microvoid coalescence and growth; c) Striation-like features

4. Conclusion

Based on the results achieved, the optimum cooling rate, austenitizing and aging temperatures, in order to have an excellent strength and good ductility together with increased fatigue endurance for 30MSV6 micro alloyed steel, can be reported as: 3.8 °C/s, 950 °C for 1 h and 600 °C for 1.5 h, respectively. This combination of optimum properties is concerned to the interlamellar spacing of pearlite, pre-eutectoid ferrite size and presence of (V,Ti)C and VC precipitates formed on grain and sub-grain boundaries or randomly distributed within the pre-eutectoid ferrite phase.

Comparing the mechanical properties of the as-received material with the ones of optimal heat treated specimen showed improvements of about 4.3%, 15.8% and 26.3% for UTS, YS and ductility, respectively. Improvement in the strength and ductility of the optimally heat treated specimen can be related to the refinement in the pre-eutectoid ferrite size, interlamellar spacing of pearlite and the formation of VC and (V,Ti) C precipitates at different sites of matrix.

TEM studies revealed that, these precipitates are non-coherent and orientation relationship of these precipitates with their surrounding matrix is a cube–cube one ([111]α//[001] precipitates).

The fatigue limit of the specimen which had experienced optimum conditions of heat treatment was 384 MPa which is about 16.6% and 24% higher than that of the fan cooled specimens and specimens cooled in insulated stainless steel cylinder, respectively. Increase in fatigue limit for optimal specimen is due to the variation in microstructure constituents and the related mechanical properties, specially, the increase in strength and ductility.

SEM characterization of fracture surfaces indicates ductile fracture. Cracks initiate by micro-void formation and coalescence, which finally propagate and cause the fractures of the specimen.

Acknowledgment

The support provided by the Iran Alloy Steel Company is gratefully acknowledged. The help extended by the technical staff engineers, Mr. Kardi, Mr. Mosavi, Mr. Rezaie and Mr. Meamari is appreciated. Also, we have to acknowledge the Science and Research Branch of Tehran, Islamic Azad University. Finally, we specially thank Mrs. Eshghi and to the Materials characterization Lab.

References

[1] A Ghosh, B Mishra, S Das, SChatterjee (2005) Microstructure, properties, and age hardening behavior of a thermo-mechanically processed ultralow-carbon cu-bearing high-strength steel. Met.Mater. Trans A. 36A: 703-713

[2] A.M.Elwazri, P.Wanjara,S.Yue (2005) Effect of prior-austenite grain size and transformation temperature on nodule size of micro alloyed hypereutectoid steels. Met.Mater. Trans A. 36A: 2297-2305

[3] Annual Book of ASTM Standards. 03.01 (2000) Standard Practice for Conducting Force Controlled Constant Amplitude Axial Fatigue Tests of Metallic Materials-E 466, ASTM, US

[4] Annual Book of ASTM Standards. 03.01 (2000) Standard Test Methods For Tension Testing of Metallic Materials-E 8M. ASTM, US

[5] ASM Handbook (1999) Properties and selection: irons, steels, and high performance alloys ASM International, US.

[6] D.F.Laurito, C.A.R.P.Baptista, MAS Torres, A.J Abdolla (2010) Microstructural effects on fatigue crack growth behavior of micro-alloyed steel. Procedia Engineering. 2: 1915-1925

[7] DK Matlock, G Krauss, JG Speer (2001) Microstructures and properties of direct-cooled microalloy forging steels. Mater.Process. Technol. 117: 324-328

[8] F.Perrard, P.Donnadieu, A.Deschamps, P Barges (2006) TEM study of NbC heterogeneous precipitation in ferrite. Philosophical Mag. 86(27): 4271-4284

[9] HR Najafi, J.Rassizadehghani, S Asgari (2008) As cast mechanical properties of vanadium/niobium micro-alloyed steels. Mater. Sci. Eng A. 486: 1-7

[10] K Tanaka, Y Akiniwa (2002) Fatigue crack propagation behavior derived from S-N data in very high cycle regime. Fatigue Fract. Eng. Mater.Struct. 25: 775-784

[11] K.W Andrews (1965) "Empirical formulae for the calculation of some transformation temperatures." JISI. 203: 721-727

[12] M.Jahazi, B.Eghbali (2001) Influence of hot forging conditions on the microstructure and mechanical properties of two micro-alloyed steels. J. Mater. Process. Technol. 113: 594-598

[13] P Marshal (1988) Development of Microstructure to Optimize Mechanical Performance of power Generation Equipment, MiCon 86: optimization of processing, properties, and service performance through microstructural control, ASTM special technical publication; 979, B.L. Bramfitt, R.C. Benn, C.R. Brinkman, G.F. Vander Voort, Eds. (American Society for Testing and Materials, Philadelphia) pp. 3-46

[14] R.D.K Misra, H Nathani, JE Hartmann, F Siciliano (2005) Microstructural evolution in a new 770MPa hot rolled Nb–Ti micro-alloyed steel. Mater. Sci. Eng A. 394: 339-352

[15] S Gunduz, A Capar (2006) Influence of forging and cooling rate on microstructure and properties of medium carbon microalloy forging steel. J. Mater. Sci. 41: 561-564

[16] S Sankaran, V SubramanyaSarma, K.A Padmanabhan (2003) Low cycle fatigue behaviour of multiphase micro-alloyed medium carbon steel: comparison between ferrite–pearlite and quenched and tempered microstructures. Mater. Sci. Eng A. 345: 328-335

[17] S Sankaran, V SubramanyaSarma, KA Padmanabhan, G Jaeger, A Koethe (2003) High cycle fatigue behavior of multiphase micro-alloyed medium carbon steel: a comparison between ferrite – pearlite and tempered martensite microstructures. Mater. Sci. Eng A. 362: 249-256

[18] S.P Bhat, M.E Fine (2001) Materials Science and Engineering A-structural Materials Properties Microstructure and Processing Mater. Sci. Eng A. 314: 90-96

[19] U.P.Singh, A.M.Popli, DK Jain, B Roy, S Jha (2003) Influence of micro-alloying on mechanical and metallurgical properties of wear resistant coach and wagon wheel steel. J. Mater. Eng. Perform. 12: 573-580

[20] Y Ochi, T Matsumura, K Masaki, S Yoshida (2002) High-cycle rotating bending fatigue property in very long-life regime of high-strength steels. Fatigue Fract. Eng. Mater.Struct. 25: 823-830